Available online at www.sciencedirect.com
SCIENCE DIRECT®
Journal of Chromatography A, 1079 (2005) 59–68
JOURNAL OF CHROMATOGRAPHY A
www.elsevier.com/locate/chroma

Review

Harnessing dielectric forces for separations of cells, fine particles and macromolecules

Carlos F. Gonzalez, Vincent T. Remcho *

Department of Chemistry, 153 Gilbert Hall, Oregon State University, Corvallis, OR 97331-4003, USA

Available online 13 April 2005

Abstract

A review of conventional dielectrophoresis on a microchip platform is presented. The benefits of miniaturization, some device geometries used to accomplish on-chip separations, and applications of these devices are discussed.

Keywords: Dielectrophoresis; Separations; Induced dipole; Polarizability

Contents

1. Introduction

Dielectrophoresis (DEP) is a separation method in which particles are segregated according to their susceptibility to a non-uniform electric field. A non-uniform electric field is generated by applying voltage across electrodes of appropriate geometry or by placement of insulating posts between a pair of electrodes. In both cases, the components are configured to spatially distort the electric field. Unlike electrophoresis where only dc voltage is used, either dc voltage or an ac waveform can be used in DEP to discriminate between different particles in a sample. By varying the frequency of the applied voltage, it is possible to induce a dipole moment in a particle and thereby cause the particle to experience a positive dielectrophoretic moment or a negative dielectrophoretic moment and cause the particle to move into a region of high potential or low potential, respectively. The first investigator of this phenomenon as a tool in separations was Pohl, with his analysis of suspended particles in an organic medium [1]. From his observations in this initial study, Pohl coined the term “dielectrophoresis” for the motion of particles within a medium arising from an induced dipole in a non-uniform electric field.

* Corresponding author. Tel.: +1 541 737 8181; fax: +1 541 737 2062.
E-mail address: vincent.remcho@orst.edu (V.T. Remcho).

0021-9673/$ – see front matter © 2005 Elsevier B.V. All rights reserved.
doi:10.1016/j.chroma.2005.03.070

Some initial devices used by Pohl to produce non-uniform electric fields were constructed by placing a wire in the center of a glass tube in which another wire was wrapped along the inner wall of the glass tube [2]. These devices required high potentials and were limited to analysis of particles 1 μm in diameter or larger due to Joule heating effects, which led to Brownian movement that countered dielectrophoretic force [3]. Benefits in decreasing the scale of dielectrophoretic devices, thereby increasing the dielectrophoretic force, were discussed by Bahaj and Bailey [4]. From their study, the following scalar relation can be derived:

$$F_{\mathrm{DEP}} \propto \frac{V^2}{L_{\mathrm{e}}^3} \tag{1}$$

where F_{DEP} is the dielectric force, V is the applied voltage and L_{e} is the length between electrodes. From Eq. (1), one can see that F_{DEP} is inversely proportional to the cube of the dimensions of the electrodes used, so by miniaturization of DEP devices the magnitude of the dielectrophoretic force exerted on a particle is increased. Another finding was that decreasing electrode size led to a reduction in Joule heating.

In recent years, with the use of semiconductor manufacturing technologies such as lithography, electron beam writing, and laser ablation, a move towards device miniaturization has been occurring. Benefits of device miniaturization include decreased consumption of reagents and sample, reduced analysis time, and the possibility of portable instrumentation.

Several different modes of microchip-based DEP exist. These modes include focusing/trapping DEP [5–7], isomotive DEP [8], traveling wave DEP [9–11], and DEP field-flow fractionation [12,13]. In this article, we will focus on "conventional" DEP in the microchip format: focusing and trapping of particles in devices that utilize parabolic electrodes, castellated electrodes, electrode arrays, and arrays of insulating posts as the geometries.

2. Theory

A force will be experienced by a dielectric particle when it is placed in a non-uniform electric field [14,15]. A non-uniform electric field is necessary to create an imbalanced force on the suspended particle in the field. This force variation can induce a dipole moment in the particle, and as long as the electric field is non-homogeneous the force imbalance can be used to move particles. For conventional dielectrophoresis, the dielectrophoretic force experienced by a particle in a non-uniform electric field can be approximated by [15]:

$$F_{\mathrm{DEP}} = 2\pi r^3 \,\mathrm{Re}[K(\omega)]\nabla E_{\mathrm{rms}}^2 \tag{2}$$

where r is the radius of the particle, ∇ is the del vector operator, and E_{rms} is the root mean square applied electric field.

$\mathrm{Re}[K(\omega)]$ refers to the real component of the Clausius–Mossotti factor [15] which is found by taking the real component of:

$$K(\omega) = \frac{\varepsilon_{\mathrm{p}}^* - \varepsilon_{\mathrm{m}}^*}{\varepsilon_{\mathrm{p}}^* + 2\varepsilon_{\mathrm{m}}^*} \tag{3}$$

where $\varepsilon_{\mathrm{p}}^*$ and $\varepsilon_{\mathrm{m}}^*$ are the complex permittivity of the particle and medium, respectively, and $\varepsilon^* = \varepsilon - \mathrm{j}\sigma/\omega$, where ε is the permittivity, j is $\sqrt{-1}$, σ is the conductivity, and ω is the angular frequency of the applied electric field.

A useful solution for $\mathrm{Re}[K(\omega)]$ which illustrates its dependency on the applied frequency is the derivation found by Benguigui and Lin [16]:

$$\mathrm{Re}[K(\omega)] = \frac{\varepsilon_{\mathrm{p}} - \varepsilon_{\mathrm{m}}}{\varepsilon_{\mathrm{p}} + 2\varepsilon_{\mathrm{m}}} + \frac{3(\varepsilon_{\mathrm{m}}\sigma_{\mathrm{p}} - \varepsilon_{\mathrm{p}}\sigma_{\mathrm{m}})}{\tau_{\mathrm{MW}}(\sigma_{\mathrm{p}} - 2\sigma_{\mathrm{m}})^2(1 + \omega^2\tau_{\mathrm{MW}}^2)} \tag{4}$$

where τ_{MW} is the Maxwell–Wagner charge relaxation time given by $\tau_{\mathrm{MW}} = (\varepsilon_{\mathrm{p}} + 2\varepsilon_{\mathrm{m}})/(\sigma_{\mathrm{p}} + 2\sigma_{\mathrm{m}})$. This factor accounts for the rate at which free charges distribute themselves along the surface of a sphere.

Eq. (2) is the first-order contribution to the dielectrophoretic force. The first-order dielectrophoretic force accounts for dipole contributions produced in a moderate non-uniform electric field [15,17–20]. The real component of the Clausius–Mossotti factor accounts for the polarization of a particle relative to the polarization of the suspending medium [15,17,18], and it is this induced dipole that will dictate the direction a polarized particle will move in a non-uniform field. Since the movement of a dielectric particle is mitigated by the complex permittivities of the particle and suspending medium, as indicated by the Clausius–Mossotti factor, it is possible to discriminate between particles based on their polarizability, and (unlike electrophoresis) separation of neutral particles is therefore attainable. The Maxwell–Wagner charge relaxation time describes how charges will accumulate on the surface of a suspended particle based on the conductivity and permittivity of the particle and suspending medium. These charges are within the suspended particle and are located at the interface with the suspending medium.

Equations for higher orders of the dielectrophoretic force have been derived and like the first-order dielectrophoretic force are frequency-dependent [16,19–21]. For this discussion, we assume that the contributions of higher-order dielectrophoretic forces are negligible which is often the case. One instance where higher-order dielectrophoretic forces do come into effect, however, is when trapping particles using a quadrupole electrode geometry [17], where the net dipole moment experienced by a particle is near zero.

3. Benefits of miniaturization

Through their experimentation utilizing a ring electrode placed above a planar electrode, Bahaj and Bailey conducted levitating DEP on divinyl benzene particles with diameters of 50 μm [3]. Though they did not conduct separations using

dielectrophoretic forces, they showed that by reduction of electrode size they could harness DEP with electrical fields produced using only a few volts.

Miniaturization of DEP devices has been beneficial in improving the effectiveness of DEP. The use of microscale electrodes allows for production of devices with more pronounced non-uniform fields [18]. Also, safety is improved because high fields can be produced by use of low voltage power supplies instead of high voltage power supplies as previously used. The sheer size of early DEP devices having machined electrodes produced appreciable heating, particularly in aqueous solutions, due to the high voltages needed to accomplish dielectrophoresis [3]. Heating effects are markedly reduced when smaller systems are employed, which reduces the effects of thermal motion and thus allows DEP to be applied to particles smaller than 1 μm which was not possible prior to the use of miniaturized devices. Also, the reduction in heating attenuates the possibility of denaturation of thermolabile analytes. This is important particularly in the analysis of biological macromolecules.

4. Particle movement in non-uniform electric fields

When a polarizable particle is subjected to an electrical field, a dipole moment will be induced in the particle regardless of whether it is charged or neutral [14,15]. If the electric field is uniform, a particle with an induced dipole moment will not move because the force experienced on the opposite sides of the particle will be identical. Charged particles too will experience a dipole and will move to their respective pole if the frequency of the applied potential is at or near zero, but will otherwise oscillate along with the applied frequency [22]. If the electric field is made non-uniform, the forces experienced on either side of the particle will be unequal. As a result, the particle will move in accordance with its polarizability relative to the polarizability of the medium and the angular frequency of the applied potential in accordance with Eq. (2) [14,15]. If the polarizability of the particle is greater than the polarizability of the medium, the particle will move towards a region of higher potential, and thereby experience a positive dielectrophoretic moment. In the case of a particle being less polarizable than the medium, the particle will migrate towards the lower potential region and experience a negative dielectrophoretic moment due to being displaced by the suspending medium towards the low-field region [14]. A visual representation of particles experiencing positive and negative dielectrophoretic moments is shown in Fig. 1.

Determination of the type of dielectrophoretic moment a particle will experience can be accomplished by calculating Re[$K(\omega)$] using Eq. (4). As previously stated, the real portion of the Clausius–Mossotti factor will dictate whether the dielectrophoretic force on a particle will be positive or negative. The Clausius–Mossotti factor is frequency-dependent because it is determined from the frequency-dependent complex permittivities of the particle and the medium [15,16,18].

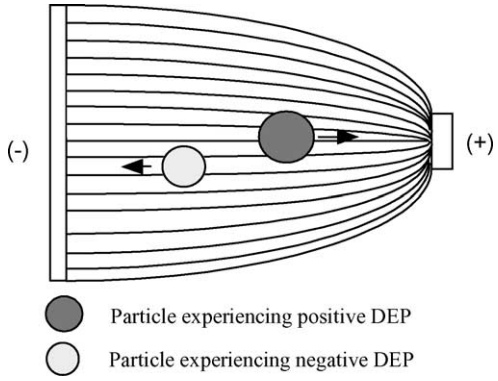

Fig. 1. Particle motion in a non-uniform electrical field. A particle that is more polarizable than the suspending medium will experience positive DEP, while a particle less polarizable than the suspending medium will migrate towards the low potential region under negative DEP.

As such, by constructing a plot of the real component of the Clausius–Mossotti factor as a function of frequency, it is possible to estimate the frequency ranges in which a particle will exhibit positive DEP and negative DEP. Fig. 2 is a plot of the real component of the Clausius–Mossotti of Fe_3O_4 in water.

When an appropriate frequency is applied across the electrodes in a dielectrophoretic device, a dipole moment is induced in particles in suspension [14,15]. If the frequency of the applied potential closely correlates to the relaxation time of the particle, defined as the time required for the induced dipole to react to the applied field, then the direction of the dipole moment experienced by the particle will reverse along with the oscillation of the ac voltage. When the frequency of the ac voltage does not correspond to the relaxation time of the particle, an induced dipole can still occur but the induced dipole will not be as great because the charge density within the particle will not have enough time to properly accumulate [14]. The influence of directionality of the applied field on the movement of a particle is not important because if the applied field is reversed then the direction of the induced dipole moment on a particle will too be reversed [14,23]. A schematic of this phenomenon is shown in Fig. 3.

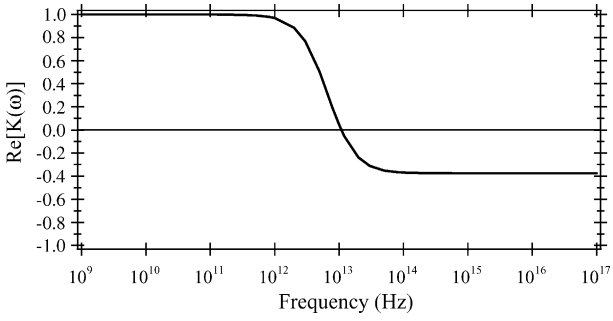

Fig. 2. Plot of Re[$K(\omega)$] vs. frequency which illustrates the frequency dependence on the polarization of Fe_3O_4 in 5.62×10^{-2} μS cm^{-1} water.

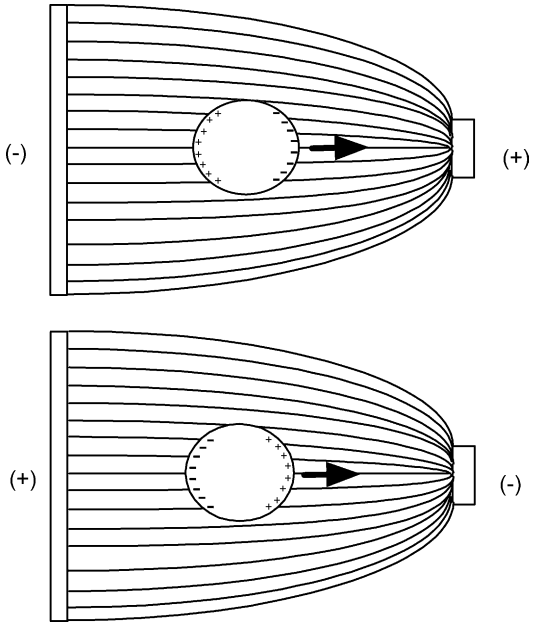

Fig. 3. Visual depiction showing that particle movement in DEP is not dependent on the direction of the applied electrical field, as shown for a particle experiencing positive DEP. For an ac applied waveform, the figure depicts an applied potential at a given point in time.

It is possible to dictate the type of DEP experienced by a particle through proper selection of the frequency. Some particles will exhibit positive dielectrophoresis through a certain frequency range and negative dielectrophoresis in another frequency range. As shown in Fig. 2, Fe_3O_4 particles would be expected to experience positive DEP in the frequency domain up to 1×10^{13} Hz and would be under negative DEP beyond 1×10^{13} Hz. The frequency at which the direction of DEP experienced by a particle changes is known as the crossover frequency. At the crossover frequency, the particle will experience no net force [18].

Careful selection of the suspending medium (and more specifically its conductivity) can be used to increase the selectivity in discriminating between different analytes as stated in the Clausius–Mossotti factor [17,18,22,24–31]. The conductivity of the medium can be altered by addition of salts. Ions present in an aqueous solution create a double layer surrounding a particle and as mentioned by Pohl [14] will have electrokinetic interactions with the particle. The thickness of the double layer can be estimated using the Debye–Hückel screening length equation [17,32]:

$$d = \left(\frac{\varepsilon_m k T}{8\pi n^\circ z^2 e_0^2} \right)^{1/2} \quad (5)$$

where ε_m is the permittivity of the medium, k is the Boltzmann constant, T is the absolute temperature, n° is the ion concentration in the bulk of the suspending medium, z is the valency of the suspending medium, and e_0 is the charge of an electron. As shown in Eq. (5), the thickness of the double layer is inversely proportional to the concentration of ions present in the suspending medium and is not dependent on the surface area or volume of the suspended particle. The close proximity of the double layer to the surface of a particle will contribute to a particles response to an oscillating electric field through electrokinetic effects [14,17]. Therefore, it stands to reason that double layer effects on the movement of a dielectric particle will be more pronounced for small particles in a low ionic strength medium.

As just stated, the DEP effects experienced by a particle will be affected by the presence of a double layer, but these added effects are especially noticed when analyzing submicron particles and macromolecules. This relation can be better understood by close examination of Eq. (2). From Eq. (2), the DEP force experienced by a particle is related to the cube of the particle radius. When dealing with particles where the size is submicrometer, the contribution of the double layer thickness will have a more profound impact on the DEP force exerted on a particle than for particles of micron and larger sizes having similar dielectric properties because of the relative contribution of the ionic double layer [26,27]. The effects of conductivity of the medium have been studied by several researchers [24–31]. Green and Morgan observed these behaviors for the study of latex spheres [24]. Huang and Pethig showed that by altering the conductivity of the solution and maintaining other conditions constant, it was possible to cause a change in the DEP behavior of yeast cells [25].

5. Dielectrophoresis geometries

5.1. Parabolic electrodes

Typical devices utilizing parabolic electrodes employ four electrodes to produce a quadrupole geometry where the electrodes are offset by 90° as shown in Fig. 4a. Voltage application is accomplished by wiring electrodes diagonally opposite one another identically [5,34–37]. Once voltage is applied after sample introduction, particles will begin to collect in regions of high or low potential depending on the dielectrophoretic moment experienced. In parabolic geometries, the potential gradient expands radially from the center of the device towards the electrode surface [24,33,34,38–41].

5.2. Castellated electrodes

As shown in Fig. 4b, castellated electrodes can be configured in two manners: directly opposite or offset. With either case, the device is wired so that every other electrode has the same voltage input [5,40,42,43]. In the case of castellated electrodes that are directly opposite each other, positive and negative dielectrophoresis regions will be found as follows [40]: particles focused in the positive dielectrophoresis region will be found between the faces of the electrodes located across from each other. Negative dielectrophoresis will congregate particles in the rectangular areas between

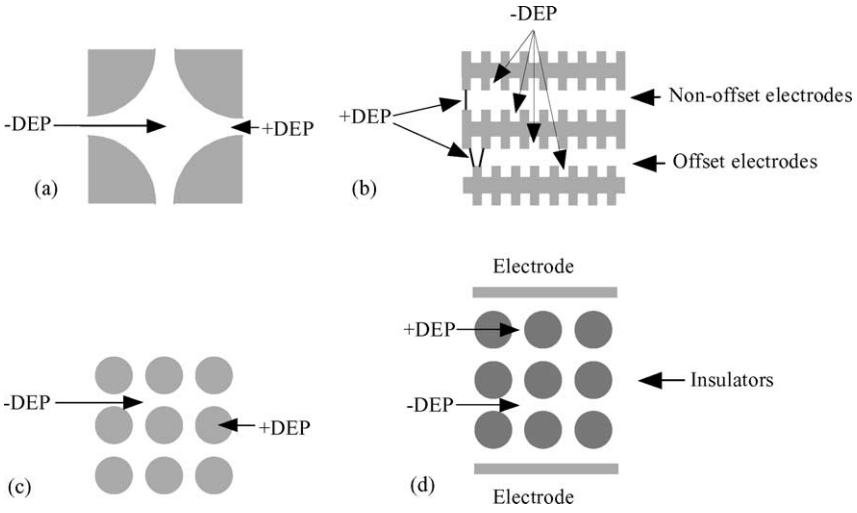

Fig. 4. Typical device geometry and regions where positive dielectrophoresis (+DEP) and negative dielectrophoresis (−DEP) are located: (a) polynomial electrode geometry; (b) castellated electrode geometry showing both non-offset and offset castellated electrodes; (c) an array of circular electrodes; (d) electrodeless geometry where regions of high and low field strength are produced by the compression of the electric field between the array of insulators.

the castellations in the electrode. Positive and negative dielectrophoresis regions for offset castellated electrodes will be found as follows [40,44]: positive dielectrophoretic particle collection again occurs in the region between castellated electrodes located across from each other, the difference being that the positive region is now found between the corners of the electrode faces. The low potential region for offset castellated electrodes is identical to that for parallel castellated electrodes (electrodes aligned directly across from each other) and therefore the negative dielectrophoresis region is located in the rectangular "wells" between electrodes.

5.3. Electrode arrays

Fig. 4c shows a common electrode array geometry. In devices containing electrode arrays, voltage applications to the electrodes vary [45,46]. One approach is to use a checkerboard pattern where electrodes having voltage applied and those that are grounded are alternated. Another possibility is to have the voltage vary in concentric squares and to have the voltage vary between ground and applied voltage with each concentric square. With electrode array geometries, the high potential region is located on the electrode surface and therefore particles experiencing a positive dielectrophoretic moment will gather on the electrode surface. Particles with a negative dielectrophoretic moment aggregate in the low potential region located in the areas surrounded by four electrodes that form a square [45,46].

5.4. Electrodeless/insulator-based devices

Fig. 4d is a representation of a dielectrophoretic device utilizing an array of insulating posts, in this case circular insulators. Unlike the previously mentioned methods of achieving focusing/trapping mode dielectrophoretic separations, devices constructed with an array of insulating posts do produce an inhomogeneous electrical field with electrodes. The non-uniform electrical field is produced by compressing the electrical field, applied by the electrodes adjacent to the insulating post, through the gaps between the insulating posts [7,47,48]. From the preceding description, it should be evident that the high potential regions will be located between the insulators where the electrical field is being compressed, as highlighted in the figure. The low potential regions are found along the axis where the applied voltage is being compressed [7,47–49].

6. Applications

Miniaturized DEP devices have successfully been used for analysis of several types of samples. These include particles [24,33,35,36,38,41,50–57], cells [6,7,25,36,37,40,42–46,48,49,57–62], and macromolecules/subcellular biological analytes [5,34,36,39,47,63–65]. Prior to listing examples, it is important to mention some potential pitfalls that may be encountered when conducting DEP separations on the microchip platform.

The first of these pitfalls deals with fluid motion that can be mistaken for DEP. Fluid motion around electrodes can be caused by electroosmotic forces [17,33,50,66–68]. In an electrolytic solution typically below 500 kHz [50], the interaction between the double layer located on an electrode surface and the electrical field will create a phenomenon known as electrode polarization. Electrode polarization occurs when a portion of the potential is lost across the double layer as the field travels from the surface of the electrode into the bulk solution. This potential decrease thereby induces a force on the ions in the double layer and creates fluid motion. Heating is also responsible for fluid movement through

electrothermal effects [33,50,69]. Electrothermal effects create a temperature gradient and are usually experienced when applying a high frequency electric field across a high conductivity medium. This temperature gradient will also create a density gradient. This established density gradient will create convection as denser fluids begin to displace fluids with lower densities. Both electroosmotic forces and electrothermal effects have the potential to create fluid motion that may overcome the dielectrophoretic forces being exerted on an analyte.

Care must be taken when selecting the conductivity of a medium when studying biological samples. First, if the conductivity of the medium is too high, the temperature increase may be sufficient to degrade biological analytes. Also, when dealing with cells care must be taken to make sure an isoosmotic environment is established as to not affect the cell wall/membrane [18].

An additional caveat is the production of free radicals through electrochemical processes [17,70–72]. Free radicals have been shown to produce changes in pH in dielectrophoretic devices [71], and these pH changes may disrupt the function of biological analytes. H_2O_2 has been formed in sugar containing solutions, and the free radicals are created from the H_2O_2 decomposition. Catalase has also been shown to increase the rate of decomposition of H_2O_2 and in most cases eliminate H_2O_2 from the system [72]. Free radicals have too been shown to react directly with analytes and degrade biological samples [73,74].

The first two examples presented are the works conducted by Green and Morgan [52], and Watarai et al. [38] and their investigations on the effects on the motion of submicron latex spheres in a non-uniform electric field. Though these studies do not directly demonstrate separations, we feel they must be mentioned because they are to our knowledge the first examples of the use of DEP forces on submicron particles. Morgan and Green used castellated electrodes with castellations spaced at 6 μm and gaps between electrodes measuring 4 μm to study 93 μm diameter carboxylate-modified latex spheres. The applied voltage used was 1 V peak-to-peak which produced a field strength of 2.5×10^8 V mm^{-1}. The suspending medium was pH 7.1 phosphate buffer with a concentration of 1 mM and conductivity of 18 μS cm^{-1}. Morgan and Green found that for the frequency range of 1 kHz–1 MHz, the particles exhibited positive DEP and migrated to the electrode tips. The particles experienced negative DEP for frequencies greater than 20 MHz and collected in the wells in the electrodes. Watarai et al. too used microparticles composed of carboxylated polystyrene latex to study the mobility of these particles due dielectrophoretic force. They used a parabolic electrode device with a quadrupole geometry with a central region of 65 μm. Aqueous suspensions were made containing 0–5.0×10^{-3} M KCl and 2.6×10^{-7} M rhodamine B to fluorescently label the spheres. The pH of the solutions were in the range of 6.08–6.80, and the conductivity of the aqueous solutions were in the range of 3.11–701 μS cm^{-1} and were adjusted by addition of KCl.

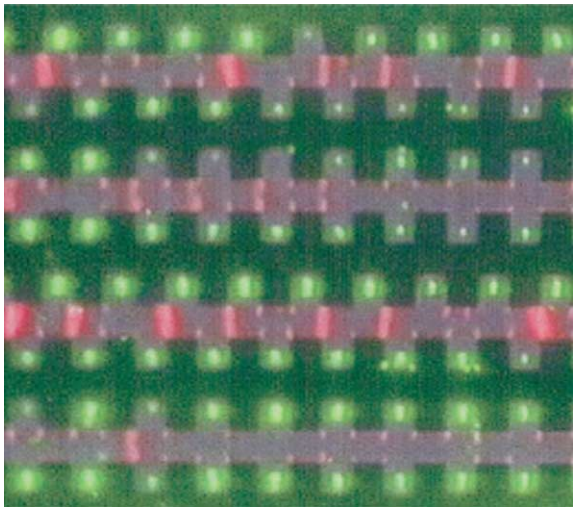

Fig. 5. A video-image capture showing 216 and 557 nm diameter latex particles separating on a 10 μm castellated electrode. The red 216 nm spheres experience positive DEP and form pearl chains between opposing electrode tips, while simultaneously the green 557 nm particles experience negative DEP and become trapped in triangular patterns in the interelectrode bays. The applied potential was 10 V peak-to-peak at a frequency of 2 MHz, and the medium conductivity was 2.5 μS cm^{-1}. Reprinted with permission from [5].

Separation of carboxylate-modified latex spheres on both non-offset and offset castellated electrodes is shown in [5]. Electrode distances used were 10 μm. Fluorescently labeled latex spheres of 216 and 557 nm diameters were suspended in an aqueous KCl solution with a conductivity of 2.5 μS cm^{-1}. Separation was accomplished using a voltage of 10 V peak-to-peak at a frequency of 2 MHz. Upon voltage application, the 216 nm particles collected in the high potential region located between electrode faces and electrode tips for non-offset and offset electrodes, respectively. The 557 nm diameter particles collected in the interelectrode gaps under negative DEP. Fig. 5 is a photograph of the above mentioned separation of 216 and 557 nm carboxylate-modified latex spheres using a castellated electrode DEP device.

Huang and Pethig [25] used parabolic electrodes to study the effects of varying the conductivity of the aqueous suspending medium on the type of dielectrophoretic force on yeast cells. The electrodes were produced from gold and had a thickness of 70 nm. The 70 nm gold electrodes were laid on a 5 nm thick chromium seed layer. The final spacing of the electrodes was 64 μm radial opening to the electrode tips. Suspensions were prepared under two different sets of conditions for the suspending medium, the first being a suspending medium composed of 280 mM mannitol with a conductivity of 3.61 μS cm^{-1}, and the second prepared with 280 mM mannitol and 1.4 mM KCl and having a conductivity of 170 μS cm^{-1}. The applied voltage was held constant at 10 V peak-to-peak and 10 kHz. The investigators found that yeast cells suspended in 280 mM mannitol experienced positive DEP, and yeast cells suspended in 280 mM mannitol and

1.4 mM KCl were focused in the central region between the electrodes.

Dielectrophoresis utilizing a castellated geometry has been shown to be a suitable extraction method for removing cancer cells from blood [58]. Non-offset castellated gold electrodes with 80 μm electrode spacing were used. A mixture of MDA 231 breast cancer cells and bovine serum was suspended in an aqueous solution consisting of 8.5% (w/v) sucrose and 0.3% (w/v) dextrose. Hemisodium EDTA was used to adjust the conductivity of the aqueous solution to 100 $\mu S\,cm^{-1}$. Upon sample introduction, a voltage of 5 V peak-to-peak at 200 kHz was applied to trap all cells under positive DEP. A flow of the suspending medium was then started at 5 $\mu L\,min^{-1}$. The frequency was lowered to 80 kHz to reduce the number of blood cells trapped on the electrodes. To further purify the breast cancer cells, the frequency was swept between 80 and 20 kHz at a rate of two times per second for 20 min to free any blood cells that have been trapped on the electrodes by the cancer cells. At the end of the 20 min sweeping cycle, cell fractions were found to be >95% pure after the cell fractions were examined using Liu's modified Wright staining.

In 1998, another example of separation of cancer cells from blood was demonstrated using DEP on a 5×5 array of electrodes [45]. The array consisted of circular electrodes composed of a 100 nm Ti–W seed layer covered with a 300 nm thick platinum layer. The electrode diameters were 80 μm and were spaced 200 μm on center. The sample analyzed consisted of epithelial carcinoma cell line (HeLa) derived from a human cervical tumor and EDTA-anticoagulated

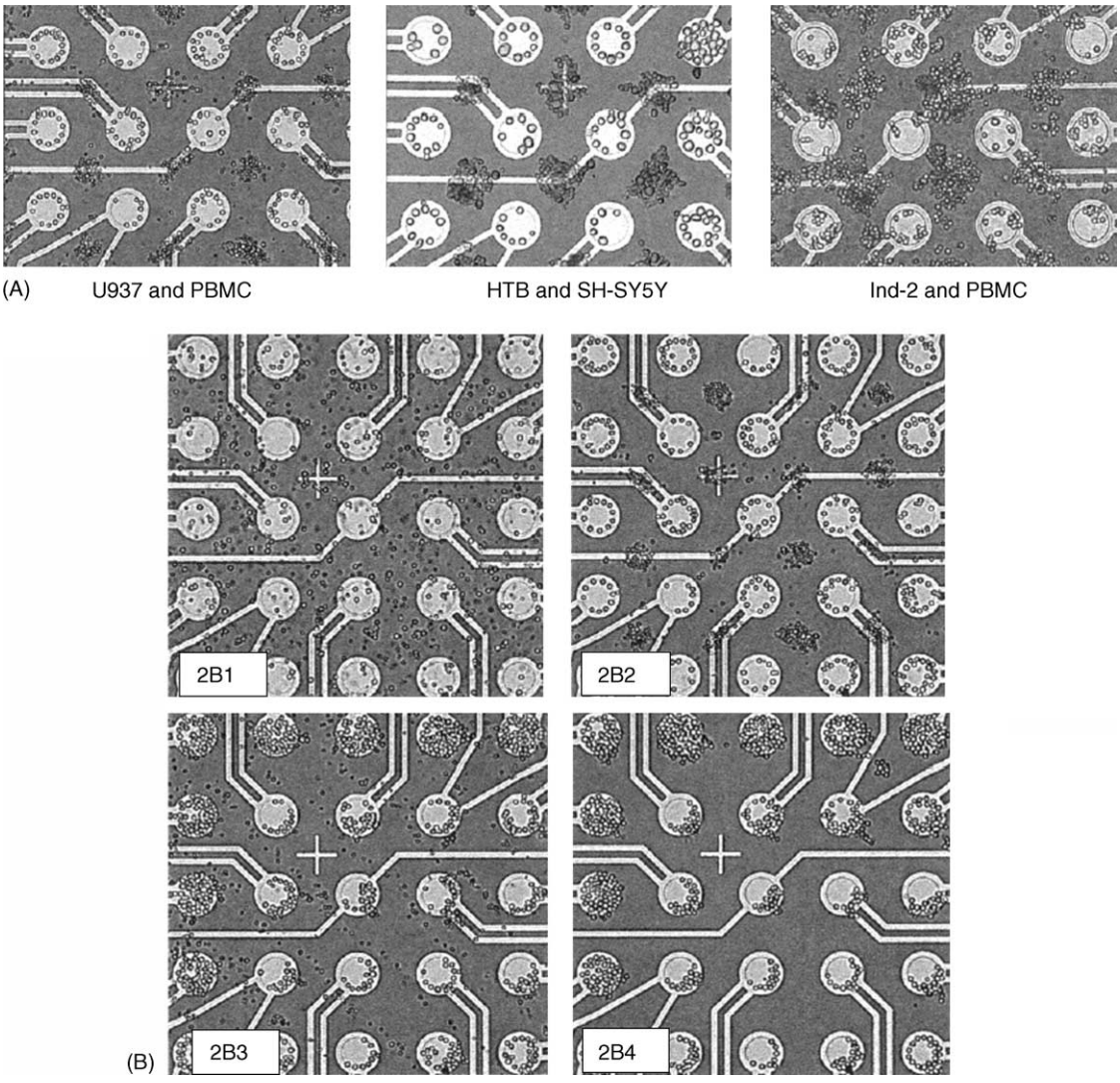

Fig. 6. (A) DEP separation of U937 and PBMC, HTB and SH-SY5Y, and Ind-2 and PBMC in a medium with conductivity of 1200 $\mu S\,cm^{-1}$ at 500, 400, and 600 kHz, respectively. (B) The procedure of DEP separation for U937 and PBMC mixture. B1: Mixture is introduced to the array. B2: U937 cells are separated from PBMC on array by dielectrophoresis 5 min after an ac voltage of 500 kHz, 7 V peak-to-peak is applied. U937 cells are collected on the electrodes and PBMC are accumulated at the space between the electrodes. B3: Buffer is introduced from reservoir to the array by fluid flow of 40 $\mu L\,min^{-1}$ while the voltage is kept on. PBMC are carried away with the fluid stream. B4: PBMC are washed off from the array and U937 cells are retained on the electrodes after 10 min of washing. Reprinted with permission from [6].

human blood cells. The separation buffer was composed of 225 nM Tris, 225 nM boric acid, and 5 nM EDTA, pH 8.2, and 250 mM sucrose. The conductivity of the separation buffer was measured to be 10 $\mu S\ cm^{-1}$. The separation voltage was 6 V peak-to-peak and the frequency was determined empirically. It was discovered that at 30 kHz, the HeLa cells experienced positive DEP and separated from the peripheral human blood cells which were under a negative dielectrophoretic moment.

Another dielectrophoretic separation of different cells lines was conducted using an array of circular electrodes [6]. Twenty-five circular platinum electrodes with diameters of 80 μm spaced at 200 μm center to center were arranged in a 5×5 geometry. The electrodes were manufactured as in the previous example and were composed of a 100 nm Ti–W seed layer covered with a 300 nm thick platinum layer. Mixtures of human glioma cell line (HTB) cells with human neuroblastoma cell line SH-SY5Y (SH-SY5Y), monocytic cells (U937) with human peripheral blood mononuclear cells (PBMC), and tax-transformed cells (Ind-2) with PBMC were studied. DEP buffer was 250 mM sucrose/RPMI 1640, and the final conductivity of the DEP buffer was 1200 $\mu S\ cm^{-1}$. Voltage was applied in a checkerboard pattern at 7 V peak-to-peak and the field frequency varied depending on the cell mixture being analyzed. Separations occurred in 3–5 min after the voltage was applied. Then cells experiencing negative DEP were flushed from the device at 40 $\mu L\ min^{-1}$ for 10 min. The voltage was then turned off the and the remainder of cells were evacuated with DEP buffer at 400 $\mu L\ min^{-1}$ for 20 s. The frequency of the applied fields were 400, 500, and 600 kHz for HTB and SH-SY5Y, U937 and PBMC, and Ind-2 and PBMC mixtures, respectively. Cell lines experiencing positive DEP were HTB, U937, and Ind-2 and were collected on the electrode surfaces, as shown in Fig. 6A. SH-SY5Y and PBMC were collected under negative DEP, also shown in Fig. 6A. Photographs of the separation of HTB and SH-SY5Y, U937 and PBMC, and Ind-2 and PBMC mixtures are shown in Fig. 6A, and the separation procedure for the U937 and PBMC mixture is illustrated in Fig. 6B.

Separation of tobacco mosaic virus (TMV) from herpes simplex virus type 1 (HSV) was demonstrated by Morgan et al. on a polynomial electrode device [5]. Electrode spacing was 2 μm for interelectrode and 6 μm in cross-center distance. The suspending medium was DI water adjusted to a conductivity of 100 $\mu S\ cm^{-1}$ using KCl. An applied voltage of 5 V peak-to-peak at a frequency of 6 MHz was used to separate TMV from HSV. Under these conditions, TMV experienced positive DEP and collected in the high-field regions, and HSV with a negative dielectrophoretic moment aggregated in the low potential region. A drawing and photograph of this separation are shown if Fig. 7a and b, respectively.

An insulator-based DEP system was used to separate and concentrate live and dead *E. coli* [7]. The insulators were produced in glass and had a height of 10 μm, diameter of 200 μm, and were spaced 250 μm on centers. The cells were suspended in DI water with a conductivity of 22.5 $\mu S\ cm^{-1}$. Direct current voltage at different voltage levels and it was found that at 16 $V\ mm^{-1}$ only live *E. coli* cells were trapped. At a potential gradient of 40 and 60 $V\ mm^{-1}$, it was noticed that both live and dead *E. coli* cells were both trapped but formed distinct bands. The separation of live and dead *E. coli* at 16, 40, and 60 $V\ mm^{-1}$ are shown in Fig. 8a–c, respectively.

Another example from the researchers at Sandia National Laboratories using insulator-based DEP is their work on separating live bacteria from water using dc voltage [48]. The separation device was again constructed of glass with circular insulators with heights of 10 and 150 μm diameters, and distanced 200 μm on centers. The suspending medium was DI water adjusted to pH 8 with 0.01 M NaOH and a conductivity of either 22 $\mu S\ cm^{-1}$ with 0.01 M KCl. Results for a total of six cell mixtures were presented. These cell mixtures were *E. coli* (BL21) and *Bacillus subtilis* (ATCC

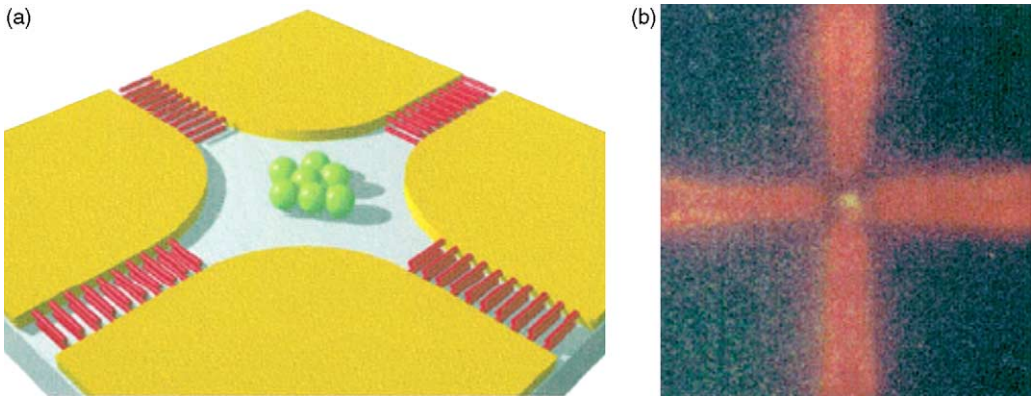

Fig. 7. A diagram and photograph illustrating the separation of TMV and HSV in a parabolic electrode. The HSV is trapped under negative DEP forces at the field minimum in the center of the electrode array, while simultaneously TMV experiences positive DEP and collects at the high-field regions at the electrode edges, resulting in the physical separation of the two particle types. This is illustrated schematically in (a); the photograph appears in (b). The TMV (labeled with rhodamine B) can be seen as a red glow in the arms of the electrodes, and the green/yellow HSV (labeled with NBD-dihexadecylamine) is visible in the center of the electrode. Both viruses were suspended in an electrolyte of conductivity 100 $\mu S\ cm^{-1}$, and the applied potential was 5 V peak-to-peak at a frequency of 6 MHz. Reprinted with permission from [5].

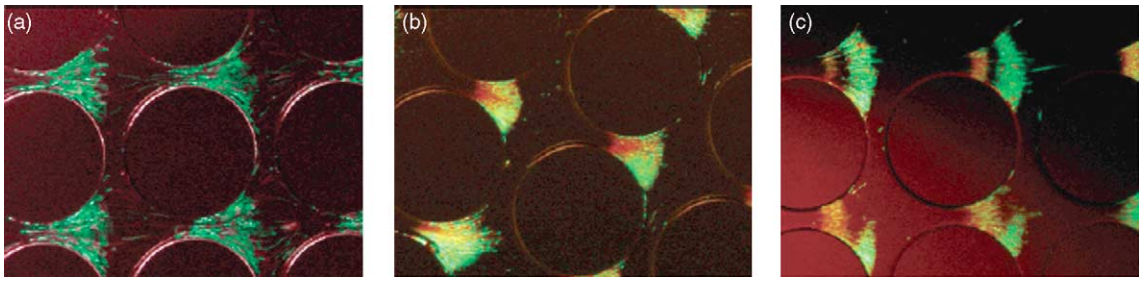

Fig. 8. Simultaneous concentration and separation of live (green) and dead (red) *E. coli* by using iDEP. Conductivity of the DI water was 22.5 μS cm^{-1}. Live *E. coli* cells were at a concentration of 6×10^7 cells mL^{-1} and were labeled green (Syto 9, Molecular Probes, Eugene, OR). Dead cells were at a concentration of 6×10^7 cells mL^{-1} and labeled red with propidium iodide (red dye, Molecular Probes, Eugene, OR). The circular posts in the arrays are 10 μm deep, 200 μm in diameter, on 250 μm centers, at 0° offset in (a) and (c), and 20° offset in (b). The electric fields applied are: (a) 16 V mm^{-1}, only live cells are trapped; (b) 40 V mm^{-1}, differential banding on live and dead cells is observed; (c) 60 V mm^{-1}, differential trapping of live and dead cells is shown by two separate bands of different color. Live cells (green) are trapped at the wider regions between the circular posts (negative DEP), and dead cells (red) exhibit less negative DEP, since they are trapped at the narrower regions between the circular posts. Reprinted with permission from [7].

Table 1
References for each particle type analyzed and the device geometry utilized

Particle type	Electrode geometry			
	Parabolic	Castellated	Electrode arrays	Electrodeless
Latex spheres	24, 33, 35, 36, 38, 39, 41, 50, 54, 56	5, 33, 50–53, 57		55
Cells	25, 36, 37, 40, 61	40, 42–44, 57–60	6, 45, 46, 62	7, 48, 49
Macromolecules/subcellular analytes	5, 34, 36, 39	40, 65	63	47, 49, 64

no. 6633), *E. coli* (BL21) and *Bacillus cereus* (ATCC no. 14579), *E. coli* (BL21) and *Bacillus megaterium* (ATCC no. 10778), *B. cereus* (ATCC no. 14579) and *B. subtilis* (ATCC no. 6633), *B. megaterium* (ATCC no. 10778) and *B. subtilis* (ATCC no. 6633), and *B. cereus* (ATCC no. 14579) and *B. megaterium* (ATCC no. 10778). For the mixture containing *E. coli* and *B. subtilis*, it was found that with a field of 50 V mm^{-1} only *E. coli* was trapped in the high potential region, and at 75 V mm^{-1} both *E. coli* and *B. subtilis* were trapped in the higher field region. *E. coli* and *B. cereus* studied at field strengths of 50 and 75 V mm^{-1} and in both of these conditions were not separated. The mixture of *E. coli* and *B. megaterium* was studied at 50 V mm^{-1} and it was found that only *E. coli* was trapped and when the field strength was raised to 90 V mm^{-1} both *E. coli* and *B. megaterium* were trapped. At a field of 25 V mm^{-1}, the fourth mixture, *B. cereus* and *B. subtilis*, only *B. subtilis* was trapped, and at a field of 75 V mm^{-1} both analytes were retained in the high-field region. *B. megaterium* and *B. subtilis* could not be separated into separate bands at 50 and 75 V mm^{-1}. The final mixture mentioned was *B. cereus* and *B. megaterium*. It was found that at a field strength of 30 V mm^{-1} only *B. megaterium* was trapped, and at 75 V mm^{-1} both *B. cereus* and *B. megaterium* were trapped into separate bands.

As noted in the discussion above, extensive analysis of suspended particles has been conducted utilizing microfabricated DEP devices. Particle types studied include but are not limited to: latex spheres, cells, viruses, proteins, and DNA. A listing of the references from this article, categorized into particle type and device geometry used in the analysis, is given in Table 1.

7. Conclusions

Recent advancements in manufacturing have allowed researchers to produce more effective dielectrophoresis devices than were possible in past years. Miniaturization has made it possible to conduct separations by applying potentials of only a few volts. Also, due to the reduction in Joule heating, it is possible to separate particles in the submicron range, which extends the utility of DEP to biological samples. Current dielectrophoretic devices have been used successfully for separation of various types of analytes, but depending on the requirements of the analysis being conducted some geometries will be of greater use than others. Both conventional dielectrophoresis and unconventional modes of dielectrophoresis have been gaining popularity as separation tools in the laboratory and commercially.

References

[1] H. Pohl, J. Appl. Phys. 22 (1951) 869.
[2] H.A. Pohl, C.E. Plymale, J. Electrochem. Soc. 107 (1960) 390.
[3] T.B. Jones, IEE Proc. Nanobiotechnol. 150 (2003) 39.
[4] A.S. Bahaj, A.G. Bailey, Proc. IEEE/IAS Annu. Meet. (1979) 154.
[5] H. Morgan, M.P. Hughes, N.G. Green, Biophys. J. 77 (1999) 516.
[6] Y. Huang, S. Joo, M. Duhon, M. Heller, B. Wallace, X. Xu, Anal. Chem. 74 (2002) 3362.
[7] B.H. Lapizco-Encinas, B.A. Simmons, E.B. Cummings, Y. Fintschenko, Anal. Chem. 76 (2004) 1571.
[8] Y. Li, K.V.I.S. Kaler, Anal. Chim. Acta 507 (2004) 151.
[9] X.-B. Wang, M.P. Hughes, Y. Huang, F.F. Becker, P.R.C. Gascoyne, Biochim. Biophys. Acta 1243 (1995) 185.
[10] H. Morgan, N.G. Green, M.P. Hughes, W. Monaghan, T.C. Tan, J. Micromech. Microeng. 7 (1997) 65.

[11] H. Morgan, A.G. Izquierdo, D. Bakewell, N.G. Green, A. Ramos, J. Phys. D: Appl. Phys. 34 (2001) 1553.
[12] X.-B. Wang, J. Yang, Y. Huang, J. Vykoukal, F.F. Becker, P.R.C. Gascoyne, Anal. Chem. 72 (2000) 832.
[13] A.I.K. Lao, Y.-K. Lee, I.-M. Hsing, Anal. Chem. 76 (2004) 2719.
[14] H. Pohl, Dielectrophoresis: The Behavior of Neutral Matter in Nonuniform Electric Fields, Cambridge University Press, New York, 1978.
[15] T.B. Jones, Electromechanics of Particles, Cambridge University Press, New York, 1995.
[16] L. Benguigui, I.J. Lin, J. Appl. Phys. 53 (1982) 1141.
[17] P.R.C. Gascoyne, J. Vykoukal, Electrophoresis 23 (2002) 1973.
[18] M.P. Hughes, Electrophoresis 23 (2002) 2569.
[19] X. Wang, X.-B. Wang, P.R.C. Gascoyne, J. Electrostat. 39 (1997) 277.
[20] M. Washizu, T.B. Jones, J. Electrostat. 38 (1996) 199.
[21] T.B. Jones, M. Washizu, J. Electrostat. 37 (1996) 121.
[22] A.D. Goater, R. Pethig, Parasitology 117 (1998) 177.
[23] R. Hölzel, F.F. Bier, IEE Proc. Nanobiotechnol. 150 (2003) 47.
[24] N.G. Green, H. Morgan, J. Phys. D: Appl. Phys. 30 (1997) 2626.
[25] Y. Huang, R. Pethig, Meas. Sci. Technol. 2 (1991) 1142.
[26] W.M. Arnold, H.P. Schwan, U. Zimmermann, J. Phys. Chem. 91 (1987) 5093.
[27] N.G. Green, H. Morgan, J. Phys. Chem. B 103 (1999) 41.
[28] Y. Huang, X.-B. Wang, R. Hölzel, F.F. Becker, P.R.C. Gascoyne, Phys. Med. Biol. 40 (1995) 1789.
[29] Y. Huang, X.-B. Wang, F.F. Becker, P.R.C. Gascoyne, Biochim. Biophys. Acta 1282 (1996) 76.
[30] V.L. Sukhorukov, W.M. Arnold, U. Zimmermann, J. Membr. Biol. 132 (1993) 27.
[31] X.-B. Wang, Y. Huang, P.R.C. Gascoyne, F.F. Becker, R. Hölzel, R. Pethig, Biochim. Biophys. Acta 1193 (1994) 330.
[32] J.O'M. Bockris, Modern Electrochemistry, vol. 2, Plenum Press, New York, 1972, p. 730.
[33] N.G. Green, A. Ramos, H. Morgan, J. Phys. D: Appl. Phys. 33 (2000) 632.
[34] S. Asokan, L. Jawerth, R.L. Carroll, R.E. Cheney, S. Washburn, R. Superfine, Nano Lett. 3 (2003) 431.
[35] S. Tsukahara, T. Sakamoto, H. Watarai, Langmuir 16 (2000) 3866.
[36] S. Tsukahara, H. Watarai, IEE Proc. Nanobiotechnol. 150 (2003) 59.
[37] K. Ratanachoo, P.R.C. Gascoyne, M. Ruchirawat, Biochim. Biophys. Acta 1564 (2002) 449.
[38] H. Watarai, T. Sakamoto, S. Tsukahara, Langmuir 13 (1997) 2417.
[39] M.P. Hughes, H. Morgan, J. Phys. D: Appl. Phys. 31 (1998) 2205.
[40] X.-B. Wang, Y. Huang, J.P.H. Burt, G.H. Markx, R. Pethig, J. Phys. D: Appl. Phys. 26 (1993) 1278.
[41] T. Müller, A. Gerardino, T. Schnelle, S.G. Shirley, F. Bordoni, B.D. Gasperis, R. Leoni, G. Fuhr, J. Phys. D: Appl. Phys. (1996) 340.
[42] P.R.C. Gascoyne, J. Noshari, F.F. Becker, R. Pethig, IEEE Trans. Ind. Appl. 30 (1994) 829.
[43] P. Gascoyne, C. Mahidol, M. Ruchirawat, J. Satayavivad, P. Watcharasit, F.F. Becker, Lab Chip 2 (2002) 70.
[44] R. Pethig, Y. Huang, X.-B. Wang, J.P.H. Burt, J. Phys. D: Appl. Phys. 24 (1992) 881.
[45] J. Cheng, E.L. Sheldon, L. Wu, M.J. Heller, J.P. O'Connell, Anal. Chem. 70 (1998) 2321.
[46] J. Cheng, E.L. Sheldon, L. Wu, A. Uribe, L.O. Gerrue, J. Carrino, M.J. Heller, J.P. O'Connell, Nat. Biotechnol. 16 (1998) 541.
[47] C.-F. Chou, J.O. Tegenfeldt, O. Bakajin, S.S. Chan, E.C. Cox, N. Barnton, T. Duke, R.H. Austin, Biophys. J. 83 (2002) 2170.
[48] B.H. Lapizco-Encinas, B.A. Simmons, E.B. Cummings, Y. Fintschenko, Electrophoresis 25 (2004) 1695.
[49] C.-F. Chou, F. Zenhausern, IEEE Eng. Med. Biol. 22 (2003) 62.
[50] A. Ramos, H. Morgan, N.G. Green, A. Castellanos, J. Phys. D: Appl. Phys. 31 (1998) 2338.
[51] N.G. Green, H. Morgan, J. Phys. D: Appl. Phys. 31 (1998) 25.
[52] N.G. Green, H. Morgan, J. Phys. D: Appl. Phys. 30 (1997) 41.
[53] M.P. Hughes, H. Morgan, Anal. Chem. 71 (1999) 3441.
[54] M. Abe, M. Orita, H. Yamazaki, S. Tsukamoto, Y. Teshima, T. Sakai, T. Ohkubo, N. Momozawa, H. Sakai, Langmuir 20 (2004) 5046.
[55] E.B. Cummings, A.K. Singh, Anal. Chem. 75 (2003) 4724.
[56] A. Docoslis, P. Alexandridis, Electrophoresis 23 (2002) 2174.
[57] R. Casanella, J. Samitier, A. Errachid, C. Madrid, S. Paytubi, A. Juárez, IEE Proc. Nanobiotechnol. 150 (2003) 70.
[58] F.F. Becker, X.-B. Wang, Y. Huang, R. Pethig, J. Vykoukal, P.R.C. Gascoyne, Proc. Natl. Acad. Sci. U.S.A. 92 (1995) 860.
[59] X.-B. Wang, Y. Huang, P.R.C. Gascoyne, F.F. Becker, IEEE Trans. Ind. Appl. 33 (1997) 660.
[60] P.R.C. Gascoyne, X.-B. Wang, Y. Huang, F.F. Becker, IEEE Trans. Ind. Appl. 33 (1997) 670.
[61] I. Ikeda, S. Tsukahara, H. Watarai, Anal. Sci. 19 (2003) 27.
[62] Y. Huang, K.L. Ewalt, M. Tirado, R. Haigis, A. Forster, D. Ackley, M.J. Heller, J.P. O'Connell, M. Krihak, Anal. Chem. 73 (2001) 1549.
[63] R.G. Sosnowski, E. Tu, W.F. Butler, J.P. O'Connell, M.J. Heller, Proc. Natl. Acad. Sci. U.S.A. 94 (1997) 1119.
[64] J.O. Tegenfeldt, C. Prinz, H. Cao, R.L. Huang, R.H. Austin, S.Y. Chou, E.C. Cox, J.C. Sturm, Anal. Bioanal. Chem. 378 (2004) 1678.
[65] W.A. Germishuizen, C. Wälti, P. Tosch, R. Wirtz, M. Pepper, A.G. Davies, A.P.J. Middelberg, IEE Proc. Nanobiotechnol. 150 (2003) 54.
[66] N.G. Green, A. Ramos, A. González, H. Morgan, A. Castellanos, Phys. Rev. E 61 (2000) 4011.
[67] A. González, A. Ramos, N.G. Green, A. Castellanos, H. Morgan, Phys. Rev. E 61 (2000) 4019.
[68] N.G. Green, A. Ramos, A. González, H. Morgan, A. Castellanos, Phys. Rev. E 66 (2002) 026305-1.
[69] B. Malyan, W. Balachandran, J. Electrostat. 51–52 (2001) 15.
[70] R.S. Nicholson, I. Shain, Anal. Chem. 37 (1965) 190.
[71] G. Fuhr, T. Müller, T. Schnelle, R. Hagedorn, A. Voigt, S. Fiedler, W.M. Arnold, U. Zimmermann, B. Wagner, A. Heuberger, Naturwissenschaften 81 (1994) 528.
[72] X. Wang, J. Yang, P.R.C. Gascoyne, Biochim. Biophys. Acta 1426 (1999) 53.
[73] C.-Y. Hsu, C.-M. Yang, C.-M. Chen, P.-Y. Chao, S.-P. Hu, J. Agric. Food Chem. 563 (2005) 2746.
[74] R.C. Murphy, Chem. Res. Toxicol. 14 (2001) 463.